RESONANT TUNNELING DIODES

Recent progress in epitaxial growth technology has made it possible to fabricate thin structures where quantum effects emerge. In these thin structures, the wave-like nature of electrons dominates the current-voltage characteristics. Electrons can penetrate barriers (tunneling), interfere, and make standing waves. A resonant tunneling diode (RTD) exploits such effects. RTDs are characterized by unique current-voltage characteristics showing negative differential resistance (NDR). They consist of extremely thin semiconductor heterolayers with thicknesses of 1 to 10 nm.

Figure 1 shows an example of the RTD structure along with the conduction band diagram. The structure consists of wide bandgap and narrow bandgap semiconductors. Typically, it is made of GaAs/$Al_xGa_{1-x}As$ system on GaAs substrate or $In_{0.53}Ga_{0.47}As/In_{0.52}Al_{0.48}As$ system on InP substrate; the GaAs and $In_{0.53}Ga_{0.47}As$ are narrow bandgap semiconductors, and the $Al_xGa_{1-x}As$ and $In_{0.52}Al_{0.48}As$ are wide bandgap ones. This structure is grown by molecular beam epitaxy (MBE) or metal-organic chemical vapor deposition (MOCVD), which can grow epitaxial layer with one-monolayer precision.

This structure contains a quantum well, which is formed when a narrow bandgap layer (well) is sandwiched by two wide bandgap layers (barriers). In the well, the energy of electrons is quantized due to the wave-like nature of electrons. (The wavelength must be such that half the wavelength (or an integer multiple) matches the thickness of the quantum well, because the electron wave is fixed at the barriers.) Electrons having an energy equal to the quantized energy levels can pass through the barriers, while those that don't have an extremely small chance of passing through. Consequently, unique current-voltage characteristics having NDR are obtained with this structure. An example of such characteristics is shown in Fig. 2. (In this figure, the anomalous step-like structures shown in the negative differential resistance region are due to the spurious effect arising from oscillation with measuring system.)

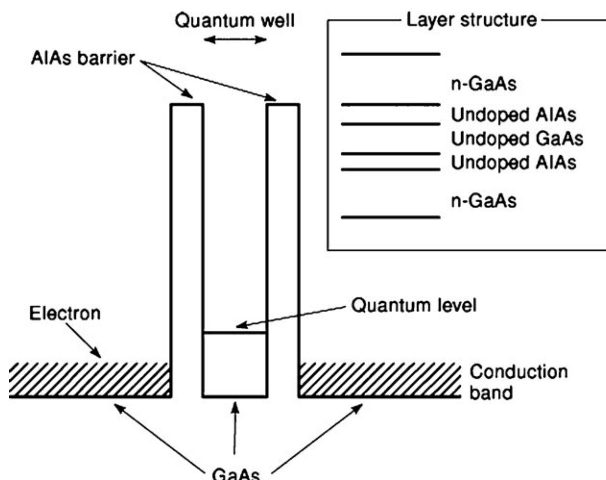

Figure 1. An example of the RTD structure with its conduction band diagram. This structure contains a quantum well, which is formed when a narrow bandgap layer is sandwiched by two wide bandgap layers.

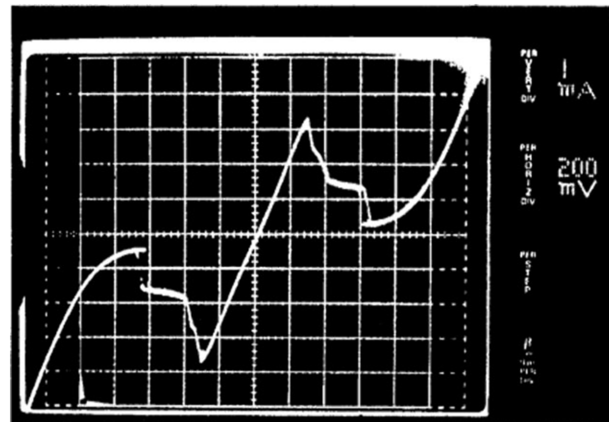

Figure 2. Current–voltage curve of the RTD. This curve is characterized by the NDR.

RTDs are attracting much attention because of their potential for high-speed operation as well as for high functionality due to the NDR. RTDs with 712 GHz oscillation (1) and 1.5 ps switching (2) have already been reported, and several functional RTD-based circuits (3), which include multiple-valued logic, a non-linear logic gate, and a neuron-like weighted-sum function (4), have also been reported. These functions reduce the number of devices used, leading to lower power dissipation. Another advantage, one of the most important ones, is that RTDs can operate at room temperature. This differentiates RTDs from most other quantum effect devices, which can operate at only cryogenic temperatures. Thus RTDs are regarded as most practical quantum effect devices for ultra high-speed analog and digital applications in the near future.

OPERATING MECHANISM

The operating mechanism of RTDs is explained here for a simple double-barrier RTD, though there are many variations of the structure. Figure 3 shows a conduction band diagram of the RTD for various applied voltages along with current-voltage characteristics. For simplicity, it is assumed that the quantum well has only one subband, which has a minimum energy of E_0. The current-voltage characteristics can be explained by the energy and momentum conservation through tunneling, as follows.

The z-direction is set perpendicular to the wafer surface. This ensures the translational symmetry in xy-plane holds during tunneling. Hence, the x and y components of the momentum, k_x and k_y, must be conserved at the tunneling, assuming where is no scattering. This indicates that the kinetic energy for z-directional motion and for motion perpendicular to the z-direction must be conserved independently. Thus the electrons in the emitter can go through the barrier into the well if the z component of the momentum k_z has a special value expressed as

$$k_{z0} = \frac{\sqrt{2m^*(E_0 - E_C)}}{\hbar}, \tag{1}$$

J. Webster (ed.), *Wiley Encyclopedia of Electrical and Electronics Engineering*. Copyright © 2007 John Wiley & Sons, Inc.

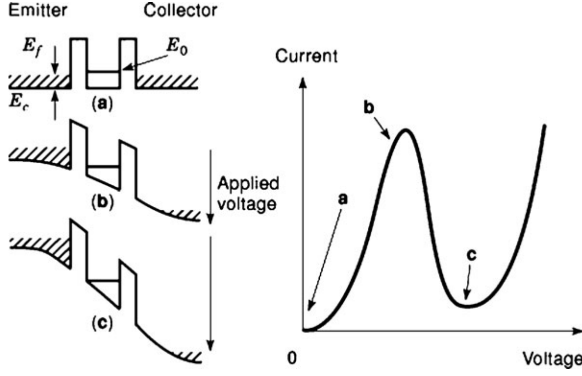

Figure 3. Conduction band diagram of the RTD for various applied voltages with current–voltage characteristics.

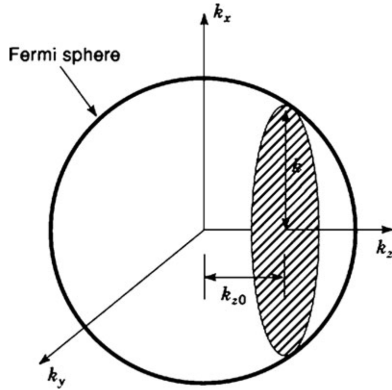

Figure 4. Fermi sphere for the degenerately doped emitter. The number of tunneling electrons is proportional to the area of the shaded disk.

where, E_C, is the energy of the conduction band edge of the emitter, m^* the electron effective mass, and $\hbar$ Planck's constant divided by 2π. The current is proportional to the number of electrons having momentum k_{z0} of the above value. This can be easily understood from Fig. 4, which illustrates the Fermi sphere for the degenerately doped emitter. Initially, the number of electrons with momentum k_{z0} is very small, or 0 at T = 0 K, when E_0 is larger than E_f. Their number then increases proportionally to the area of the shaded disk in Fig. 4 when $E_c < E_0 < E_f$. The electrons in the disk are in the resonant state. The area of the disk, πk^2, is expressed as

$$\pi k^2 = \frac{2\pi m^*(E_F - (E_0 - E_C))}{\hbar^2}. \tag{2}$$

In the simple approximation that ignores the band bending, E_C is linearly dependent on the applied voltage. This means current increases linearly with increasing the applied voltage. Then, the number of electrons abruptly decreases when E_0 drops under E_c. Finally, non-resonant current increases with increasing applied voltage beyond this point. The result is the current-voltage characteristics shown in Fig. 3.

EFFECTS OF SCATTERING

Here, let us briefly consider the effects of scattering. Scattering destroys phase coherence and breaks the transition rule. Possible scattering centers include impurities, phonons, electrons, and interface roughness. Taking scattering into account in RTD theory is difficult and is still an evolving problem.

From a qualitative point of view, scattering in the well, which breaks the phase coherence of electrons, doesn't change the operating mechanism discussed above, if the scattering rate is not large enough to prevent energy-level formation. This is because the mechanism depends only on the fact that the electrons tunnel into the 2-dimensional state in the well. It is called "sequential tunneling" when the scattering rate is large enough to destroy all coherence before electrons leave the well (5).

On the other hand, scattering plays an important role in determining peak and valley currents quantitatively (6). In particular, it has been reported that scattering due to interface roughness has a significant effect on those currents (7). The interface roughness breaks the translational symmetry in the *xy*-plane, which results in broader resonance, and hence a larger valley current.

OPERATION SPEED

One of the most significant advantages of RTDs is their extremely high operation speed. In discussing the limit of the operation speed, it is important to differentiate two response times: the so-called "tunneling time" and the "RC-time". The former is the time it takes electrons to tunnel through the RTD structure, and is related to quantum mechanics. The latter is the time required to charge the capacitance of the RTD, and is related to circuit theory.

Let us first consider the tunneling time (8). Suppose that the electric field in the RTD structure changes from the non-resonant to resonant state at a certain time t_0. The amplitude of the wave function in the quantum well changes to its steady state value in response to this change. The tunneling time is the time required for this change. This time is of the order of the resonant-state life time, t_{life}, or the escape time, which is the time it takes an electron in the quantum well to escape from it. From simple theory, this time is determined by the energy level width Γ as

$$\tau_{\text{life}} = \frac{\hbar}{\Gamma}. \tag{3}$$

The energy level width Γ is determined as the half-width of the transmission probability function through the resonant state. Roughly speaking, Γ exponentially decreases with increasing barrier thickness and height. This means a shorter tunneling time can be obtained with thinner and lower barriers, though there is a trade-off against the peak-to-valley ratio. This time determines the fundamental speed limit for ideal RTDs, and it can be as short as 0.1 ps.

However, various non-idealities in the real RTDs affect the tunneling time. These non-idealities include barrier asymmetry, interface roughness, and inelastic scatter-

Figure 5. Equivalent circuit of the RTD. This circuit consists of a voltage–dependent current source, a voltage–dependent capacitor, and a series resistor.

ings. Several theoretical and experimental studies have been devoted to clarifying the tunneling time of RTDs. A time-resolved photoluminescent measurement using ultra-short pulses (9) has revealed that the escape time from a 2-dimensional well agrees reasonably well with eq. (3). On the other hand, the tunneling time was estimated from the high-frequency characteristics of quantum-well-base transistors (10). These devices were heterojunction bipolar transistors with a base layer consisting of a resonant tunneling double barrier structure. The results again showed that the tunneling time is in reasonable agreement with eq. (3). The resonant life time described in eq. (3) is a useful guideline for designing high-speed RTDs, though further studies to clarify the tunneling time in real systems are necessary. In addition to the tunneling time, the transit time across the collector depletion layer affects RTD response when large spacer layers are used.

Next, we will discuss the operation speed limited by RC-time. In most applications, the operation speed of RTDs is limited not by the intrinsic tunneling time but by the charging time of RTD capacitance. RTDs are well described by the equivalent circuit in Fig. 5. This circuit consists of a voltage-dependent current source $I_{RTD}(V)$, a voltage-dependent capacitor $C_{RTD}(V)$, and a series resistor R_s. Here, the parallel combination of $I_{RTD}(V)$ and $C_{RTD}(V)$ represents an intrinsic RTD, and the R_s is the sum of series resistances such as the contact resistances. An investigation of the capacitance $C_{RTD}(V)$ is extremely important in determining the maximum operation speed of RTD circuit. A schematic diagram of the capacitance-voltage curve is shown in Fig. 6 with the current-voltage curve as a reference. The capacitance of the RTD is extracted from the results of microwave S-parameter measurements (11). In short, there are two main points. First, the capacitance is roughly equal to that calculated from the undoped spacer layer and the depletion layer of the device, except for the voltage near the peak. Second, there is an anomalous peak structure in the NDR region, as shown in Fig. 6. This peak is due to resonant electrons accumulated in the well. This must be taken into account to discuss operating speed precisely. Note that $I_{RTD}(V)$ and $C_{RTD}(V)$ do not depend on the frequency when the frequency is sufficiently smaller than the intrinsic limit determined by the lifetime discussed above.

Here, consider the operation speed limits for two typical applications. The first is an oscillator (12). The NDR of RTDs can act as the basis for a very fast and simple oscillator. The maximum frequency of the oscillation, f_{max}, is

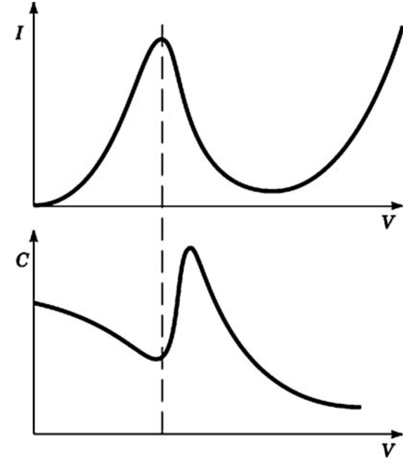

Figure 6. Schematic diagram of the capacitance–voltage curve with a current–voltage curve as a reference. An anomalous peak structure is shown in the NDR region.

expressed as

$$f_{max} = \frac{1}{2\pi C}[\frac{-G_{max}}{R_S} - G_{max}^2]^{1/2}, \tag{4}$$

where, G_{max} is the maximum negative conductance in the NDR region and C is the capacitance at the voltage where G_{max} is obtained. This is the frequency above which the dynamic current through the capacitance masks the NDR. Consequently, no oscillation occurs above this frequency. This frequency can be extremely high, for example, 1.24 THz (1).

The second example is the switching time for the resistance-load RTD circuit (13). Figure 7 shows the load diagram and the switching mechanism of the circuit. A small pulse applied to the bias terminal makes the circuit switch from off to on. This switching time can be calculated from the equivalent circuit model, and is approximated to be a few times RC, where C is the average capacitance in the NDR region and the R is the negative resistance. Extremely short switching times of 1.7 (14) and 1.5 ps (2) have been reported for InAs/AlSb and InAs/AlAs RTDs, respectively.

It is worth noting here about the advantages of RTDs compared to Esaki diodes. The *I-V* curves of Esaki diodes show NDR similar to RTDs, and several applications similar to RTDs have been studied. The one of most important advantages of the RTD is the ability to obtain a high peak

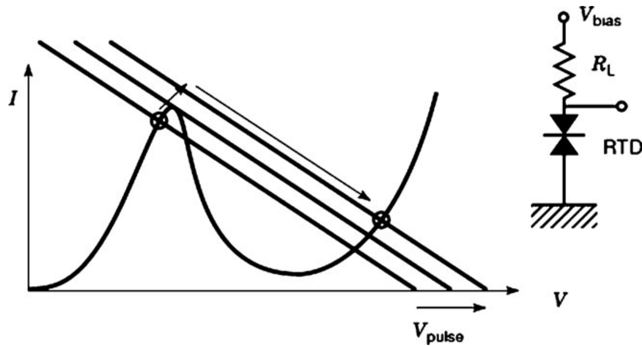

Figure 7. Load line diagram of the resistive load RTD switch circuit. The circuit switches its state in response to a small pulse (V_{pulse}) applyed to the bias voltage. A small pulse applied to the bias terminal makes the circuit switch from off to on.

current density with a relatively low capacitance. (For example, an extremely high current density of 6.8 GA/m^2 is obtained with a capacitance of about 1.5 mF/m^2 (2).) This is possible because the current density of RTDs can be increased by changing the barrier and the well thicknesses, and this can be achieved without decreasing depletion layer thickness. On the other hand, one must increase impurity density to decrease tunnel barrier (=depletion layer) thickness in order to increase current density in Esaki diodes. Consequently, the maximum operation speed of RTDs can be much higher than that of Esaki diodes. Furthermore, RTDs can avoid degradation observed in Esaki diodes due to impurity diffusion at the highly-doped pn-junction.

VARIATIONS OF RTDS

Several variations of RTDs have been studied recently. First, the one variation is an RTD with more than two barriers. The purpose of using multiple barriers is to obtain multiple peak *I-V* curve, which can be used for application for multiple-valued logic (15). Also, the triple-barrier structures have been used to make a sharp peak. This is because the first quantum well plays the role of a filter (16). Several materials other than GaAs/AlAs or InGaAs/InAlAs systems have also been studied. Particularly, the AlSb/GaSb/InAs systems is attracting much attention because of its unique band lineups. Two different structures have been proposed for this material system (17, 18). One is the AlSb/InAs/AlSb double barrier quantum well structure, which has a band diagram similar to that of AlAs/GaAs. This heterostructure has a larger barrier height than AlAs/GaAs, so a larger peak-to-valley (P/V) current ratio can be obtained. The other is the resonant intervalley tunneling diode (RITD), which exploits the type II band alignment of the An AlSb/GaSb/InAs system. (The conduction band minimum of InAs is lower than the valence band maximum of GaSb). RITDs consist of a GaSb well sandwiched by AlSb barriers with InAs emitter/collector layers. In the GaSb well, quasi bound states are formed in the valence band. This allows electrons in the emitter to tunnel through the valence band state of GaSb to the collector. In this structure, the bandgap of GaSb blocks the leakage current at the valley voltage. Consequently, an extremely high P/V ratio of more than 20 is possible at room temperature.

The implementation of RTDs with a Si-based material system have been reported recently. Various structures, such as SiO_2/Si, SiGe/Si, Al_2O_3/Si, and CdF2/CaF_2/Si RTDs were reported for future integration of RTDs on Si substrate (19–21). Until now, only limited performances are obtained for these systems (low P/V ratio, low peak current density). This is due to the higher electron mass in Si compared to that of the compound semiconductors. Further effort should be necessary to realize high performance Si-based RTDs. However, the emergence of high-performance Si-based RTDs would have an extremely significant impact, because highly functional circuits using them could be implemented in Si VLSIs.

APPLICATIONS

Several possible RTD applications that exploit the NDR characteristics are now being developed. Though most of them are similar to those once proposed for Esaki diodes, progress in related device technology and the ultra high-speed potential of RTDs open up new possibilities.

The most attractive applications are microwave/millimeter wave analog circuits (12). They include the oscillator shown in the previous section, a frequency multiplier, a mixer, and a trigger (22). Recent interests on THz wave technology revives the attention to the RTD oscillators. Most recently, an RTD oscillator integrated with stacked-layer slot antennas have been proposed, and demonstrated 1 THz signal generation using harmonic oscillation (23).

The frequency multiplier uses the folded *I-V* curve due to the NDR. Because of this *I-V* curve, the output current shows two or three peaks for one half of applied voltage swing. This results in highly efficient frequency multiplication. Several circuits have also been proposed for digital applications (3). The latching function due to the bistability of RTD circuits is the basis for most of these applications. A typical example of such a circuit is a (multiple-valued) memory, which uses RTDs connected in series or parallel with appropriate load.

An RTD has only two terminals, which restricts the use of resonant tunneling phenomena. Adding a control terminal to RTDs extends their usability to a variety of applications. The most straightforward way to do this is to merge RTD with conventional transistors to make a composite device. This approach has been used to build resonant tunneling bipolar transistors (RTBTs) (3), resonant tunneling hot electron transistors (RHET) (24), and gated RTDs. The RTBTs have a resonant tunneling structure at the emitter/base junction region or in the base. A RHET is similar to RTBT and has a resonant tunneling structure at the emitter of the hot electron transistor. Consequently, these devices have negative transconductance in emitter-grounded transistor characteristics. These non-linear input-output characteristics can be applied to several circuits, such as an XOR logic gate with only one transistor. On the other hand, gated RTDs have Schottky or junction gates around

the emitter to control RTD area, and show an NDR with controlled peak current. These devices are used for a functional logic gate called a MOBILE (monostable-bistable transition logic element) (4), and are useful in investigating the physics of very small tunneling structures (25).

The other and more practical way to add the control terminal is to connect RTDs with ordinary transistors to make parallel or series circuits. Integration of RTDs with transistors is necessary in order to do this, but this has a significant advantage beyond merely adding a control terminal. One can use both of RTD circuits and ordinary transistor circuits according to its merits and demerits. Integration of RTDs with HEMTs or bipolar transistors have been proposed, and several circuits have been also reported using such devices (26–28). The MOBILE can also be fabricated with these combinations, and recently various circuits applications have been reported (29).

In summary, RTDs are excellent candidates the high-speed and low-power applications of the near future, and vigorous efforts to build and perfect them shall continue.

BIBLIOGRAPHY

1. E. R. Brown, J. R. Sderstrm, C. D. Parker, L. J. Mahoney, K. M. Molvar, and T. C. McGill, Oscillations up to 712 GHz in InAs.AlSb resonant-tunneling diodes, *Appl. Phys. Lett.* **58**: 2291–2293, 1991.
2. N. Shimizu, T. Nagatsuma, T. Waho, M. Shinagawa, M. Yaita, and M. Yamamoto, In0.53Ga0.47As/AlAs resonant tunneling diodes with switching time of 1.5 ps, *Electron. Lett.* **31**: 1695–1697, 1995.
3. F. Capasso, S. Sen, F. Beltram, and A. Y. Cho, Resonant tunnelling and superlattice Devices: Physics and circuits, In F. Capasso (ed.), *Physics of Quantum Electron Devices*, Berlin: Springer-Verlag, 1990.
4. K. Maezawa, T. Akeyoshi, and T. Mizutani, Functions and applications of monostable-bistable transition logic elements (MOBILEs) having multiple-input terminals, *IEEE Trans. Electron Devices* **41**: 148–154, 1994.
5. S. Luryi, Hot-electron injection and resonant-tunneling heterojunction devices, In F. Capasso, and G. Margaritondo (ed.), *Heterojunction Band Discontinuities*, Amsterdam: North-Holland, 1987.
6. S. Datta, *Electronic Transport in Mesoscopic Systems*, New York: Cambridge University Press, 1995.
7. P. Roblin, R. C. Potter, and A. Fathimulla, Interface roughness scattering in AlAs/InGaAs resonant tunneling diodes with an InAs subwell, *J. Appl. Phys.* **79**: 2502–2508 (1996) .
8. D. K. Ferry, Theory of resonant tunnelling and surface superlattices, In F. Capasso (ed.), *Physics of Quantum Electron Devices*, Berlin: Springer-Verlag, 1990.
9. M. Tsuchiya, T. Matsusue, and H. Sakaki, Tunneling sscape rate of electrons from quantum well in double-barrier heterostructures, *Phys. Rev.* **59**: 2356–2359, 1987.
10. T. Waho, S. Koch, and T. Mizutani, Experimental analysis of resonant tunneling transit time using high-frequency characteristics of resonant tunneling transistors, *Superlattices and Microstructures* **16**: 205–209, 1994.
11. N. Shimizu, T. Waho, and T. Ishibashi, Capacitance anomaly in the negative differential resistance region of resonant tunneling diodes, *Jpn. J. Appl. Phys.* **36**: L330–L333, 1997.
12. T. C. L. G. Sollner, E. R. Brown, W. D. Goodhue, and H. Q. Le, Microwave and millimeter-wave resonant tunneling devices, In F. Capasso (ed.), *Physics of Quantum Electron Devices*, Berlin: Springer-Verlag, 1990.
13. S. K. Diamond, E. zbay, M. J. W. Rodwell, D. M. Bloom, Y. C. Pao, and J. S. Harris, Resonant tunneling diodes for switching applications, *Appl. Phys. Lett.* **54**: 153–155, 1989.
14. E. zbay, D. M. Bloom, D. H. Chow, and J. N. Schulman, 1.7ps, microwave, integrated-circuit-compatible InAs/AlSb resonant tunneling diodes, *IEEE Electron Device Lett.* **14**: 400–402, 1993.
15. T. Tanoue, H. Mizuta, and S. Takahashi, A triple-well resonant-tunneling diode for multiple-valued logic application, *IEEE Electron Device Lett.* **9**: 365–367, 1988.
16. T. Nakagawa, H. Imamoto, T. Kojima, and K. Ohta, Observation of resonant tunneling in AlGaAs/GaAs triple barrier diodes, *Appl. Phys. Lett.* **49**: 73–75, 1986.
17. L. F. Luo, R. Beresford, and W. I. Wang, Resonant tunneling in AlSb/InAs/AlSb double-barrier heterostructures, *Appl. Phys. Lett.* **53**: 2320–2322, 1988.
18. J. R. Sderstrm, D. H. Chow, and T. C. McGill, New negative differential resistance device based on resonant interband tunneling, *Appl. Phys. Lett.* **55**: 1094–1096, 1989.
19. K. Yuki, Y. Hirai, K. Morimoto, K. Inoue, M. Niwa, and J. Yasui, Novel Si resonant tunneling Device, Extended Abstracts of the 1994 International Conference on Solid State Devices and Materials, *Yokohama*, 319–321, 1994.
20. S. L. Rommel, T. E. Dillon, M. W. Dashiell, H. Feng, J. Kolodzey, P. R. Berger, P. E. Thompson, K. D. Hobart, R. Lake, A. C. Seabaugh, G. Klimeck and D. K. Blanks, Room temperature operation of epitaxially grown $Si/Si_{0.5}Ge_{0.5}/Si$ resonant interband tunneling diodes. *Appl Phys Lett* **73** 15, pp. 2191–2193, 1998.
21. S. Watanabe, T. Sugisaki, Y. Toriumi, M. Maeda and K. Tsutsui, Fabrication of Fluoride Resonant Tunneling Diodes on V-Grooved Si(100) Substrates, *Jpn. J. Appl. Phys.*, Vol.**45**, No. 6A, pp. 4934–4938, 2006.
22. L. Yang, S. D. Draving, Dan E. Mars, and Mike R. T. Tan, A 50 GHz broad-band monolithic GaAs/AlAs resonant tunneling diode trigger circuit, *IEEE J. Solid-State circuits* **29**: 585–595, 1994.
23. N. Orihashil, S. Hattoril, S. Suzukil and M. Asada, Experimental and Theoretical Characteristics of Sub-Terahertz and Terahertz Oscillations of Resonant Tunneling Diodes Integrated with Slot Antennas, *Japanese Journal of Applied Physics* Vol.**44**, No. 11, pp. 7809–7815, 2005.
24. N. Yokoyama, S. Muto, H. Ohnishi, K. Imamura, T. Mori, and T. Inata, Resnoant-tunneling hot electron transistors (RHET), In F. Capasso (ed.), *Physics of Quantum Electron Devices*, Berlin: Springer-Verlag, 1990.
25. P. H. Beton, M. W. Dellow, P. C. Main, L. Eaves, and M. Henini, Magnetic-field dependence of the electrical characteristics of a gated resonant-tunneling diode, *Phys. Rev. B* **49**: 2264–2264, 1994.
26. A. C. Seabaugh, E. A. Beame III, A. H. Taddiken, J. N. Randall, Y.-C. Kao, Co-integration of resonant tunneling and double heterojunction bipolar transistor on InP, *IEEE Electron Device Lett.* **14**: 472–474, 1993.
27. J. Shen, S. Tehrani, H. Goronkin, G. Kramer, R. Tsui, An Exclusive-NOR based on resonant interband tunneling FET's, *IEEE Electron Device Lett.* **17**: 94–96, 1996.
28. K. J. Chen, K. Maezawa, T. Waho, M. Yamamoto, Device technology for monolithic integration of InP-based resonant tun-

neling diodes and HEMTs, *IEICE Trans. Electron.* **E79-C**: 1515–1524, 1996.

29. K. Maezawa and A. Foerster, Quantum Transport Devices Based on Resonant Tunneling, In R. Waser (ed.), *Nanoelectronics and Information Technology*, Wiley-VCH, Berlin, 2003.

KOICHI MAEZAWA
University of Toyama, 3190 Gofuku, Toyama-shi, Japan, 930-8555